J. Earth Syst. Sci. (2024)133 175
https://doi.org/10.1007/s12040-024-02397-x

Anisotropy of magnetic susceptibility and rock magnetism of high-grade rocks from Eastern Ghats Mobile Belt, India: Constraints to tectonics

Solanky Das[1,*], M Venkateshwarlu[2], Supriya Mondal[1], Saurodeep Chatterjee[3] and Debesh Gain[1]

[1] *Department of Geological Sciences, Jadavpur University, Kolkata 700 032, India.*
[2] *CSIR–National Geophysical Research Institute, Hyderabad 500 007, India.*
[3] *Department of Geology, Rajiv Gandhi University, Itanagar 791 112, India.*
[*] *Corresponding author. e-mail: dassolanky14@gmail.com*

MS received 16 October 2023; revised 19 January 2024; accepted 16 May 2024

The present study deals with the Fe–Ti oxides, rock magnetic and anisotropy of magnetic susceptibility (AMS) carried out to determine the magneto-mineralogical characteristics and the nature of the magnetic fabrics of the high-grade metamorphic rocks from Chilka Lake area, Eastern Ghats Mobile Belt (EGMB), India. Petrography depicted the presence of both primary and secondary magnetite and titano-magnetite as the chief magnetic minerals. Different generations of magnetite were found in these rocks corresponding to different conditions of temperature that prevailed during their oxidation, having tectonic implications depicting the crustal upliftment. Thermomagnetic analysis, isothermal remanent magnetization (IRM), hysteresis loops and backfield IRM demagnetisation show the presence of ferrimagnetic minerals of different origin. The magnetic domain is determined by Day plot, using the remanence and coercivity values from hysteresis curves, dominated by stable single domain (SSD), which reveals the potentiality to record the ancient magnetic field. AMS studies unravelled the nature of the magnetic fabrics in the region. The magnetic susceptibility ellipsoids are dominantly oblate as revealed from the P_j–T_j shape plots. The magnetic lineation is highly variable which states the multiple phased tectono-metamorphic conditions. The similarity between the magnetic and mesoscopic fabrics in the granulite is significant, whereas the anorthosites result from felsic magmatism, which occurred after the deformational phases and thus did not record any mesoscopic tectonic significance.

Keywords. AMS; EGMB; high-grade metamorphic rocks; rock magnetism; tectonics.

---

1. Introduction

The EGMB of India consists of outcrops of multiply deformed, high-grade metamorphic rocks belonging to granulite facies of Grenvillian age (1.1–0.95 Ga) (Bhattacharya *et al.* 1998; Krause *et al.* 2001; Dobmeier and Raith 2003). The granulites are intruded by several anorthosite massifs (Chatterjee 1960; De 1969), Balugaon and Rambha anorthosite massifs being most characteristic (Ray 1952; Perraju 1960, 1973; De 1969). Stable magnetization is common in the massif anorthosites

Published online: 02 September 2024

(McEnroe *et al.* 2002; Robinson *et al.* 2002, 2004; Brown and McEnroe 2004, 2008, 2012). Rock magnetic and AMS studies are very important on these rocks for correlation to regional tectonics. AMS is a useful tool to study about deformation and tectonics, which can be obtained from the various statistical parameters and orientation attributes related to AMS (Borradaile and Alford 1987; Borradaile 1991; Parés and van der Pluijm 2002; Till *et al.* 2010; Ferré *et al.* 2014; Fodor *et al.* 2020; Agarwal *et al.* 2021). One of such high-grade metamorphic terrain is EGMB, which is studied by many workers over last few decades mostly using petrology, geochronology, geochemical studies, etc. (Sengupta *et al.* 1999; Dobmeier and Simmat 2002; Krause *et al.* 2001 and references there in). However, no detailed magnetic studies have been done in this terrain. Magnetic fabrics are reported from few metamorphic terrains, such as Oddanchatram anorthosite, Tamil Nadu (Satyanarayana *et al.* 2003), Southern Granulite terrain (Mondal *et al.* 2009), Chotonagpur Granite Gneissic layered complex (Chatterjee *et al.* 2018b) and Kondapalle–Pangidi layered complex (Gain *et al.* 2022). The present attempt is related to both rock magnetic and AMS studies of the granulite rocks of the EGMB and the anorthosite intrusives at Balugaon and Rambha. The aim of the study is to identify the different magnetic remanence carrier residing in the rocks and tectonic implications by different generations of magnetic minerals. Another important identification is the magnetic fabric analysis by anisotropy of magnetic susceptibility (AMS) in relation to the deformational history of the study area.

2. Geology, sampling and methods

The Proterozoic EGMB is a high-grade metamorphic belt along the eastern coast of the Indian peninsula which extends for about 1600 km from Cuttack in Odisha to Nellore in Andhra Pradesh. The area under study is in and around Chilka Lake, Odisha and is located along the NE boundary of the Eastern Ghats Belt (figure 1). The EGB has a trend of NE–SW covering an area of about 50,000 km^2. The massif-type anorthosites have widespread occurrences with the adjacent high-grade metamorphic rocks of the Proterozoic time (Anderson 1969; Isachsen 1969; Sighinolfi and Gorgoni 1975; Berrang 1996). The tectonic evolution around the Chilka Lake area is known (Dobmeier and Simmat 2002). The anorthosite massifs are surrounded by high grade metamorphic rocks such as khondalite (Walker 1902), charnockite, leptynite (Sen 1987), mafic granulite, calc-silicate granulites. All these rocks underwent high-temperature to ultra-high temperature (HT-UHT) metamorphism (Dobmeier and Simmat 2002).

The present study is conducted within a latitude range of 19°27′–19°58′N and longitude 85°00′–85°25′E. In and around Chilka Lake area (CHL), a total of 38 sites were visited, amongst which 25 sites were selected for the detailed study. One oriented block sample, along with a few chip samples, were collected from each site. A total of 25 block samples were collected from individual sites in the studied area. Among these, 12 sites are from granulites, 9 from anorthosite and 4 from leptynite. Mesoscopic structural data were also collected from the exposed structural features in the field. Each of the samples was drilled out at the Rock Cutting Laboratory, Jadavpur University, Kolkata, India, using a non-magnetic drill bit. From each block sample at least 6 cores of 2.2 cm height and 2.54 cm diameter were drilled out. A total of 180 cores were drilled for magnetic measurements. AMS studies of these cores were carried out using Bartington Susceptibility Meter (MS-2). MS-2 Susceptibility Meter (Bartington, UK) was used for the low-field AMS analysis at 0.46 kHz. It works in synchronous operation with the AMS-Bar software, which measures susceptibility in 18 different orientations. On the basis of these 18 different orientations, the principal susceptibility axes' direction, along with corresponding susceptibility values and different parameters, are obtained as outcomes in the Geophysical Laboratory, Department of Geological Sciences, Jadavpur University, Kolkata, India. Based on this analysis, magnetic data and respective parameters are obtained.

From each of the block samples, a portion was mortared into powder for the rock magnetic analysis at the Palaeomagnetism Laboratory, CSIR – National Geophysical Research Institute (NGRI), Hyderabad, India. The rock magnetic measurements were conducted using an advanced variable field translation balance (AVFTB). Thermo-magnetic, isothermal remanent magnetization (IRM) and hysteresis loops were determined from the rock magnetic analysis. For the petrological study, polished thin sections were prepared from the collected chip samples. The optical information and the textural relationship were studied under a

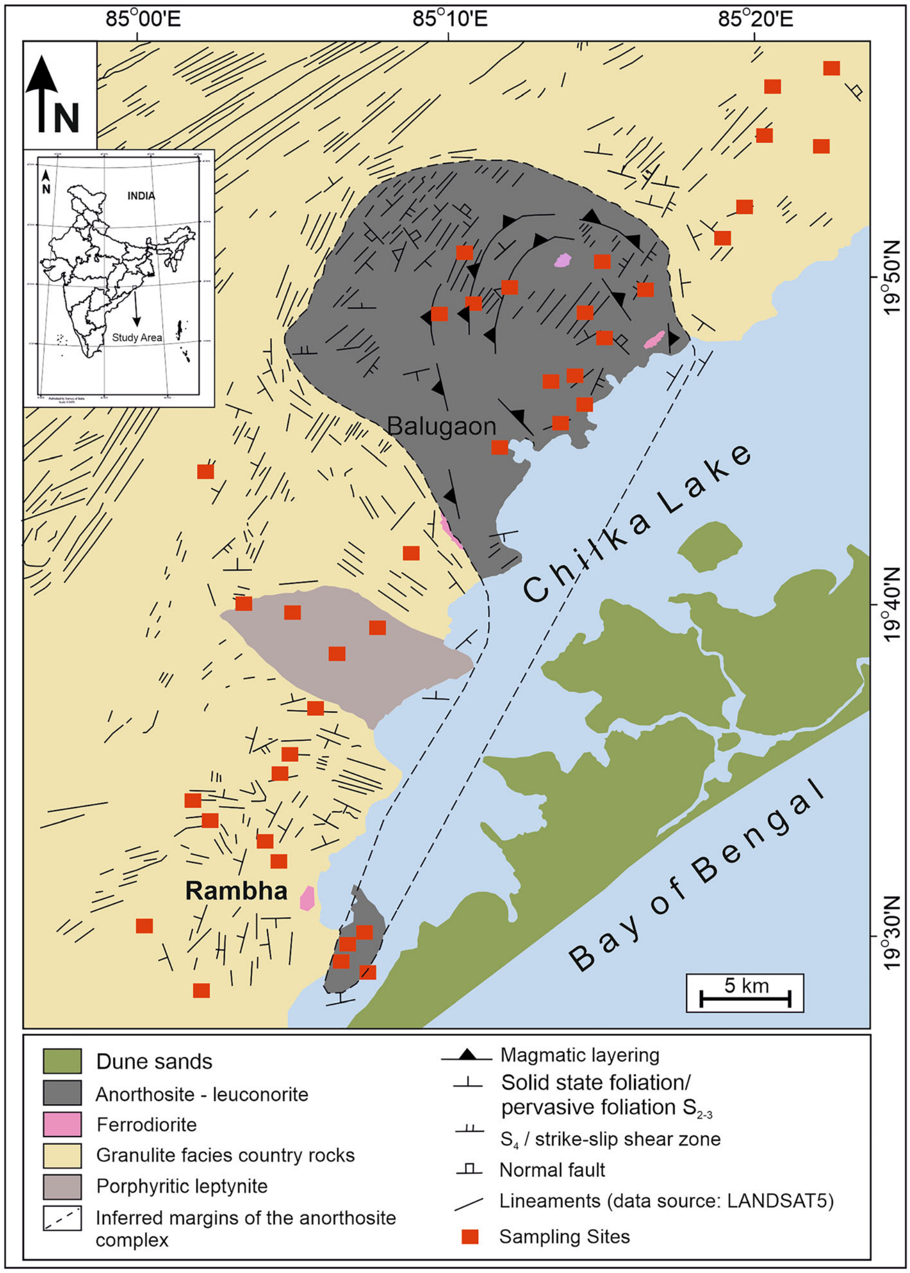

Figure 1. General geological map of Balugaon–Rambha anorthosite massif and its surrounding granulites, Eastern Ghats Mobile Belt, India (after Dobmeier and Simmat 2002).

petrological microscope at Jadavpur University. Oxide phases were studied under reflected light setup.

3. Mineralogy and rock magnetic results

3.1 *Petrography*

Mineralogy and the textural relationship between silicates and opaque minerals are identified under the transmitted light. The granulite is composed of plagioclase, orthopyroxene, k-feldspar with minor quartz and biotite (figure 2a). The feldspar and pyroxene both are present as phenocrysts and as finer grains throughout the interstitial spaces forming granoblastic texture in the orthopyroxene granulites (figure 2b). Coronal garnet is also observed here (figure 2b). Anorthosite contains ∼70% plagioclase (figure 2c). Prominent triple junction of the plagioclase phenocrysts is also seen, depicting granoblastic texture (figure 2d). Anorthosite is composed of coarse-grained feldspar and can even preserve stable magnetisations due to the presence of crystallographically oriented Fe–Ti

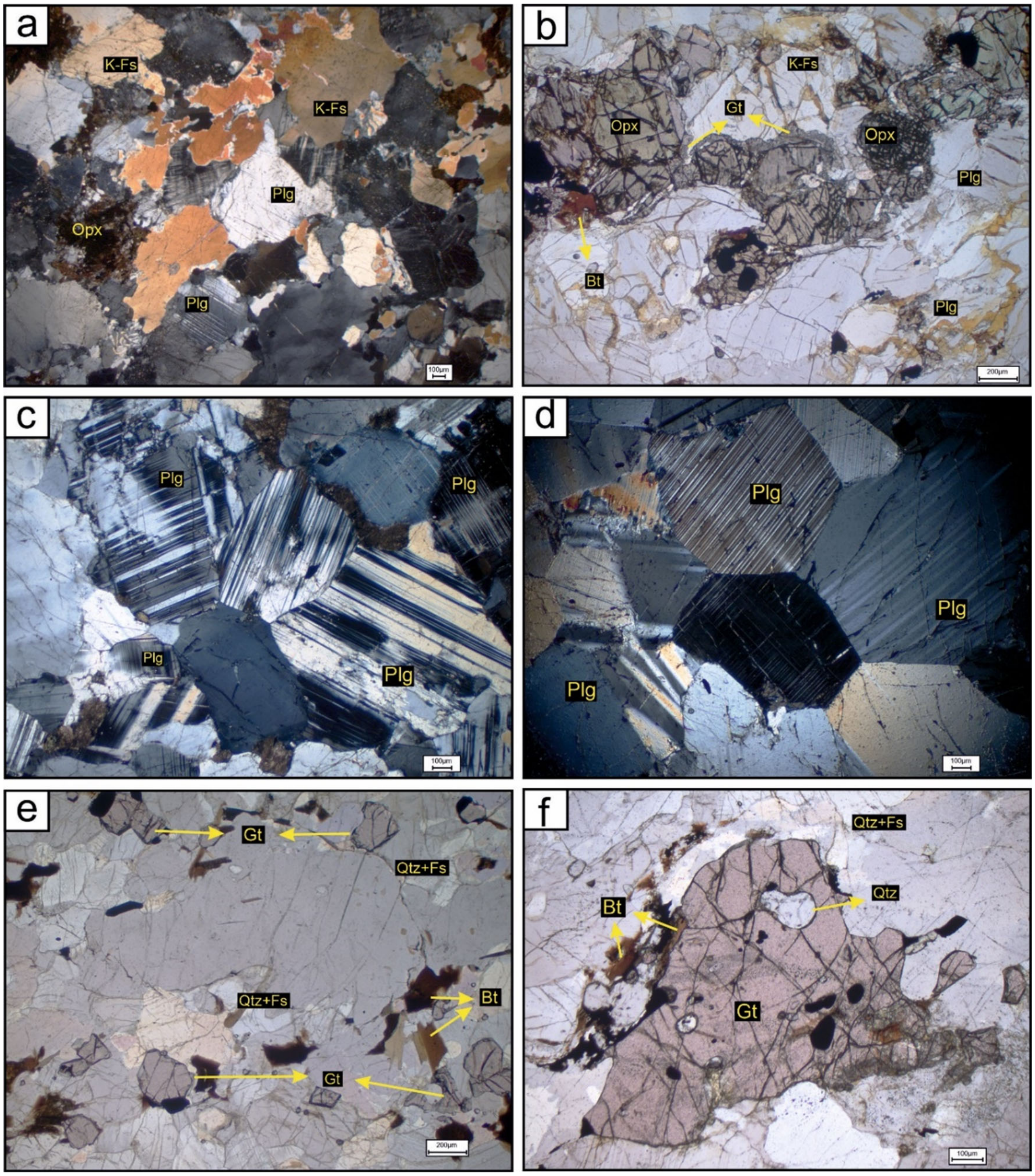

Figure 2. Photomicrographs showing different rock types encountered in the study area. **(a)** Orthopyroxene granulite displaying granoblastic texture defined by orthopyroxene, plagioclase, k-feldspar with minor biotite and opaque (XPL); **(b)** Orthopyroxene granulite displaying granoblastic texture defined by orthopyroxene, plagioclase, k-feldspar with minor biotite and coronal garnet (PPL); **(c)** Anorthosite defined by ample amount of plagioclase feldspar (XPL); **(d)** Plagioclase porphyroblast shows triple junction (XPL); **(e)** Alternate band of Qtz+Fs and opq+bt in leptynite (PPL), and **(f)** Porphyroblastic garnet showing inclusion of quartz and opaque, presence of biotite and opaque along the grain boundary (PPL). PPL: Plane polarised light, XPL: Cross polarised light.

oxides as primary coarse grains, as inclusions in silicate minerals and as secondary oxide grains, which make it an important element in the palaeomagnetic study. Leptynite consists of plagioclase, garnet, biotite, and quartz in decreasing order. Gneissic banding is observed at some places (figure 2e) in leptynite. Opaque minerals are also present throughout, along grain boundaries and along fractures of silicate grains. Silicates, as well as opaque minerals, are present as inclusions within garnet (figure 2f). Opaque minerals are present in all the rock samples in different proportions.

3.2 *Magnetic mineralogy*

In the studied rock samples, both high-temperature (Haggerty 1976) and low-temperature (Johnson and Hall 1978) oxidation of Fe–Ti oxide grains are present. In the study area, fresh oxide grains with prominent grain boundaries indicate high-temperature oxidised grain, C-1 stage (figure 3a, b) present in granulite and anorthosite. In anorthosite, ilmenite lath present within the titano-magnetite grain denoting the C-3 stage of oxidation, i.e., a higher oxidation stage (figure 3c) is also present. Thick ilmenite lath sandwiched within Ti-rich layers in granulite depicts the later stage of C-3 (figure 3d). In the case of low-temperature oxidation, fresh grain without any crack indicates 'Stage-1' (figure 4a), where the grain has not experienced any low-temperature oxidation. 'Stage 2' (figure 4b) was identified by the development of microscopic cracks (Akimoto *et al.* 1984) all around the periphery of the grain during the initiation of low-temperature oxidation. The stage of oxidation increases to 'Stage-3' (figure 4c) when the cracks start to migrate inward towards the centre from the periphery, resulting in the cracks filling up by silicates, Stage-4 (figure 4d). Iron oxides are also seen along the grain boundaries (figure 5a), along cleavage planes and along fractures of silicates (figure 5b). They are the secondary Fe–Ti oxides which look like small broken grains. More than one generation of oxides are seen in the samples.

3.3 *Magnetic hysteresis studies*

The hysteresis loops were obtained by applying alternative magnetic fields to the samples until saturation was attained. Hysteresis loops obtained from the samples exhibit a saturated nature with moderately high remanence (figure 6a, b, e, f) and an unsaturated magnetization nature along with low or no remanence (figure 6c, d) defined by separate curves. Characteristic curves show elongation with an undersaturation of magnetisation and very low to low remanence indicating paramagnetic and ferrimagnetic minerals present in the same sample (figure 6c, d). Curves (figure 6a, b, e, f) show saturation of magnetization and remanence indicating ferrimagnetism. M_{rs}/M_s values fall between 0.03 and 0.41 with an average of 0.17. H_{cr}/H_c, the ratio of remanent coercivity and coercivity of remanence lies between 0.13 (for leptynite) and 1.03 (for anorthosite) with an average of 0.88 (figure 7). The magnetic hysteresis parameters are plotted in a representative diagram called Day plot (Day *et al.* 1977), with the variations in magnetic domain states (figure 7).

3.4 *IRM acquisition curves and coercivity spectra*

The IRM acquisition curve depicts the saturation obtained by applying a magnetic field to the samples with gradually increasing strength. After a

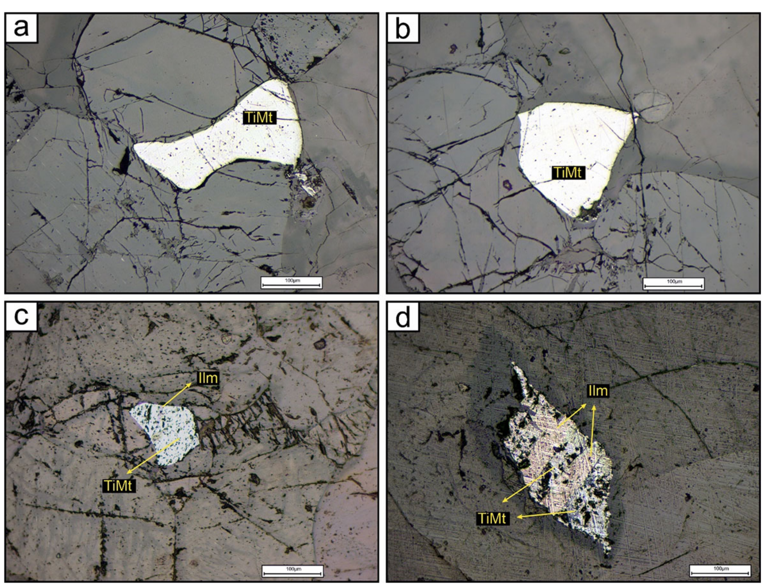

Figure 3. **(a)** Homogeneous C-1 phase, present within grain interstitial space (irregular shape), **(b)** homogeneous C-1 phase with euhedral shape as an entity of granoblastic texture; **(c)** C-3 with exsolved thin ilmenite lamellae developed within Ti–Fe oxide (XPL), and **(d)** later stage of C-3 with thick ilmenite lath sandwiched with Ti-magnetite. PPL: Plane polarised light, XPL: Cross polarised light.

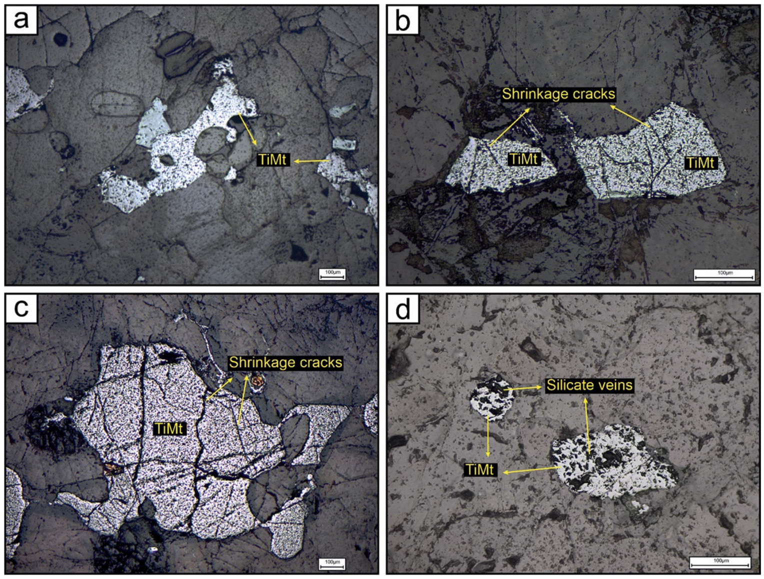

Figure 4. Low-temperature oxidized phases include **(a)** homogeneous Stage-1 (PPL); **(b)** Stage-2 with moderately developed shrinkage cracks (PPL); **(c)** Stage-2 to Stage-3 with prominent shrinkage cracks (XPL), and **(d)** Stage-3 with cracks replaced by silicates (XPL). PPL: Plane polarised light, XPL: Cross polarised light.

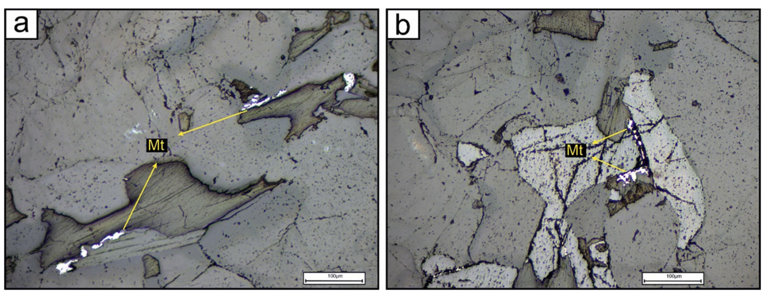

Figure 5. The Fe–Ti oxides also present as ultrafine grains. **(a)** Secondary oxide grains along the silicate grain boundary and **(b)** along the fracture plane. PPL: Plane polarised light, XPL: Cross polarised light.

sharp rise, the curve starts to saturate below 300 mT, and the saturation was obtained for some samples CHL 6, CHL 8, CHL 11 and CHL 19 (figure 8a, b, c, d). All the samples have a coercivity <10 mT (figure 8e, f, g, h). The nature of the obtained curves resembles the presence of ferrimagnetic minerals. Both the IRM and coercivity spectra point towards soft magnetic minerals (viz., magnetite or Ti-magnetite).

3.5 *Thermo-magnetic studies*

The thermo-magnetic study is done to know the Curie point and change in the behaviour of the magnetic minerals within the sample during both the heating and cooling cycles. Identification of the principal magnetic minerals present in the samples is possible by observing the nature of the thermomagnetic curves obtained and by observing the Curie temperature (T_c), where the saturation remanence falls to zero. From the thermomagnetic curves of the CHL samples, it is observed that in most of the curves, the magnetization shows a sharp drop in between ∼560° and 580°C during the heating cycle (the red line). The nature of the curves from CHL 5, CHL 11 and CHL 3 (figure 9a, b, e) depict the presence of ferrimagnetic minerals. Both the heating and cooling curves crosscut each other (figure 9d); this cross-over is attributed to the exsolution of the Ti-rich lamella, which is ilmenite (from petrographic studies), making the host Fe-rich. The curve (figure 9c) shows both paramagnetic and ferrimagnetic nature, the paramagnetic nature of the curve tends to stretch the T_c at ∼680°C and the ferrimagnetic nature at 580°C. Paramagnetism is indicated in different CHL samples (figure 9c, f).

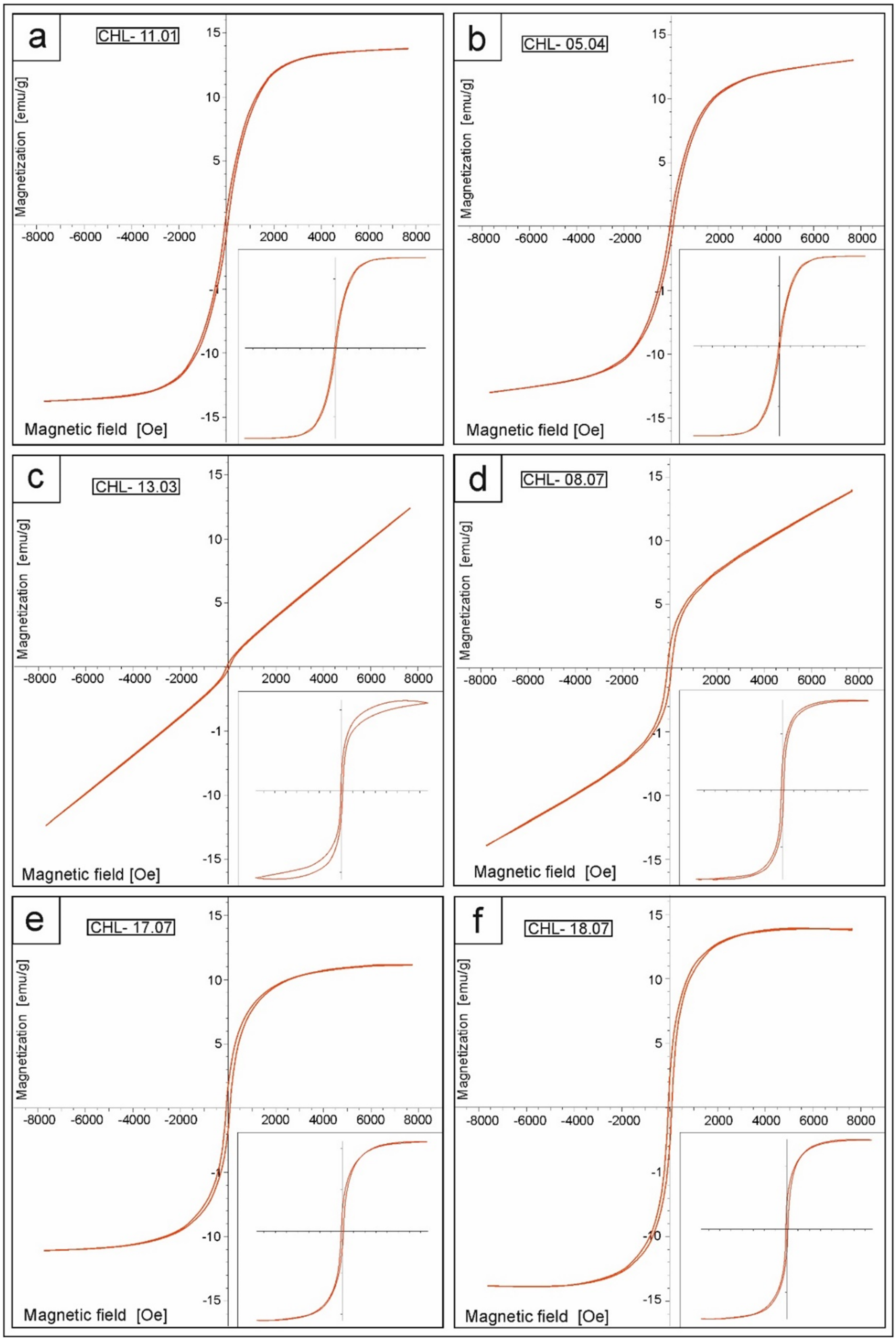

Figure 6. Strong field hysteresis loops for representative samples. Insets represent the hysteresis loops after paramagnetic correction.

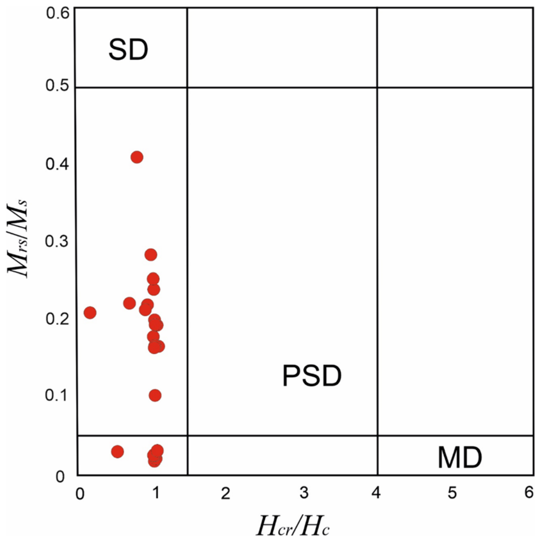

Figure 7. Distribution of the domain states of Ti-magnetite in different rocks of Balugaon and Rambha anorthosite massifs along with surrounding granulites (Day *et al.* 1977).

4. Anisotropy of magnetic susceptibility studies

AMS is used to determine the grain alignments within the rock with an ambient stress field during its formation and the prolonged journey till date. All the parameters related to AMS depending upon the rock types are stated in table 1. The mean values of individual AMS parameters are also stated there.

The mean magnetic susceptibility (K_m) of the CHL samples varies from 2.44 $\times$ 10^{-5} to 704 $\times$ 10^{-5} SI units. The L ranges from 0.6 to 1.9 and F ranges from 1.1 to 2.1. The degree of anisotropy (P_j) is almost uniform in all the samples; values fall between 1.1 and 2.6, and the shape parameter (Tj) shows positive values except in some of the samples. All the P_j values range within a certain limit; the mean value of the individual four sections is >1.05 (table 1), which is the verge value for magnetic fabric which is tectonically controlled (Dvorak and Hrouda 1975; Tarling and Hrouda 1993; Chatterjee *et al.* 2018a; Mondal *et al.* 2022). However, the P_j–T_j plots (Jelinek 1981) range from prolate to oblate but mostly oblate in nature (figure 10). The P_j–K_m plot (figure 11) is plotted to see the susceptibility change related to the corrected anisotropy.

4.1 *Magnetic fabrics*

The lower hemisphere equal area plots of all principal susceptibility axes of the different sectors of rock types are more of dispersed all throughout than clustered (figure 12). The α_{95} value for both K_1 and K_3 also range widely (table 1). The trend of magnetic lineation and pole-to-magnetic foliation varies lithologically (figures 13 and 14). The magnetic lineation has high plunge and variable trend. The mean of magnetic lineation of different rocks is NW–SE for northern sector granulites, almost E–W for anorthosite, NE–SW in leptynite and NE–SW in southern sector granulites. The magnetic lineation map (figure 15) and magnetic foliation map (figure 16), which represent the magnetic fabric of the study area are provided.

5. Discussions

5.1 *Magnetic mineralogy and remanence carriers*

The major rock types of the study region are granulite, anorthosite and leptynite. There are different generations of Fe–Ti oxides present along with their different stages of oxidations. Both low-temperature (<350°C) and high-temperature (>600°C) primary oxides are observed.

A higher temperature oxidation has been reached as evidenced by the homogeneous oxide grain of the C-1 stage (figure 3a, b). The grain with ilmenite lath indicates the C-3 stage (figure 3c), and even later stage of C-3 with thick ilmenite bands sandwiched inside the Fe-rich layer indicates higher oxidation (figure 3d). According to Das *et al.* (2012), M_2–D_2 is the peak metamorphic event of the area, i.e., the peak metamorphic assemblage in the studied high-grade metamorphic rocks is attained during this second stage of metamorphism, which is, in turn, coeval with the D_2 deformational event. So, the high-temperature Fe-oxides may be syn-tectonic during M_2, the highest temperature and highest pressure attained by the rocks. In granulite facies, the high-temperature phases occur during the prograde metamorphism (Wang *et al.* 2015). During post-peak metamorphism, i.e., the retrograde process or D_3 the low temperature oxides may have formed, which suffered low-temperature upliftment related oxidation (Akimoto *et al.* 1984). Different stages of low-temperature oxides, Stage-1, Stage-2 and Stage-3 (figure 4) are shown. Garnets with oxide inclusions (figure 2f) indicate that those oxides are primary. Some silicates and garnets are highly fractured and have decomposed during D_3. The high-temperature

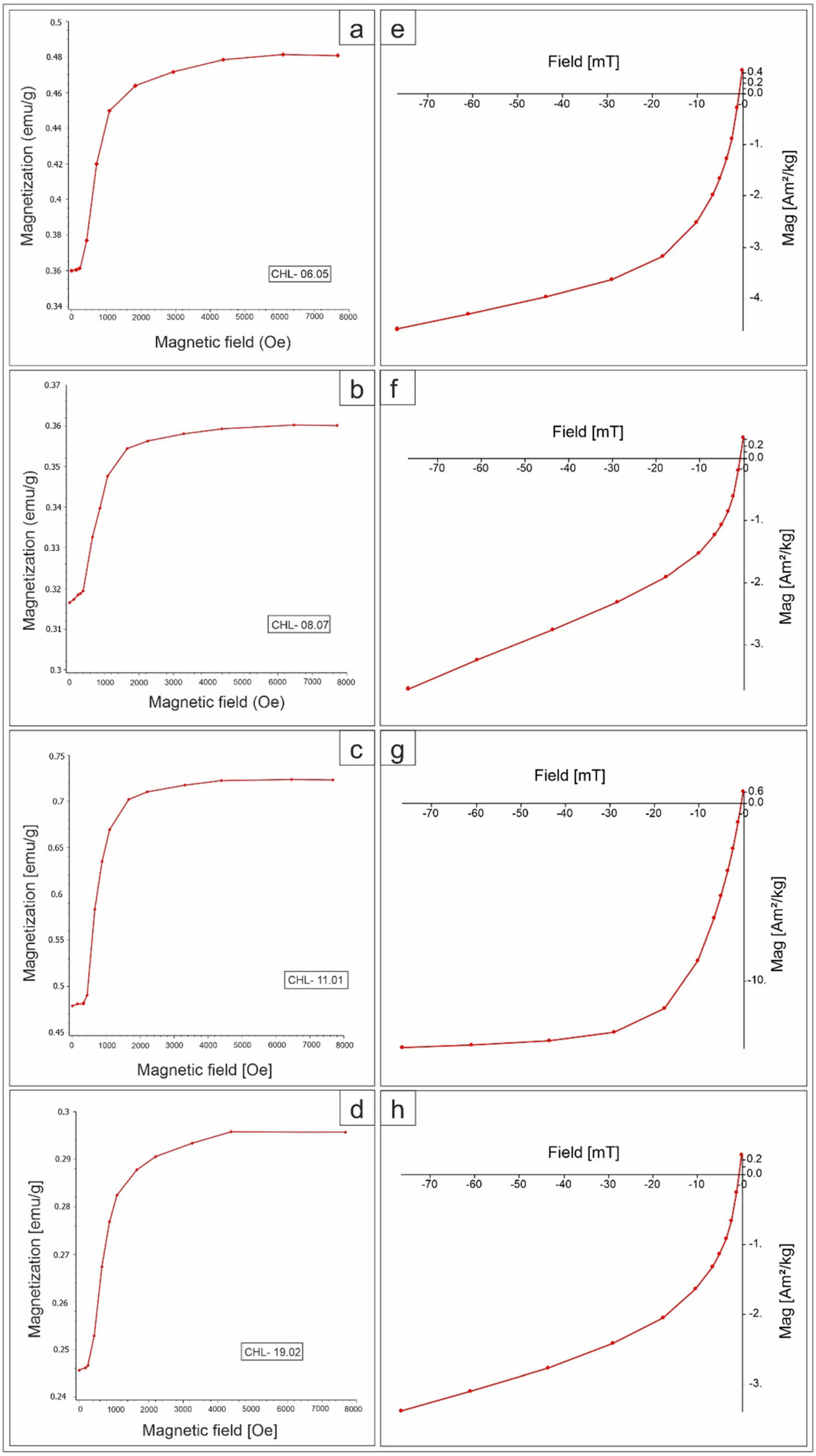

Figure 8. Isothermal remanent magnetization (IRM) acquisition curves and corresponding coercivity spectra (backfield IRM demagnetisation) for representative samples of CHL.

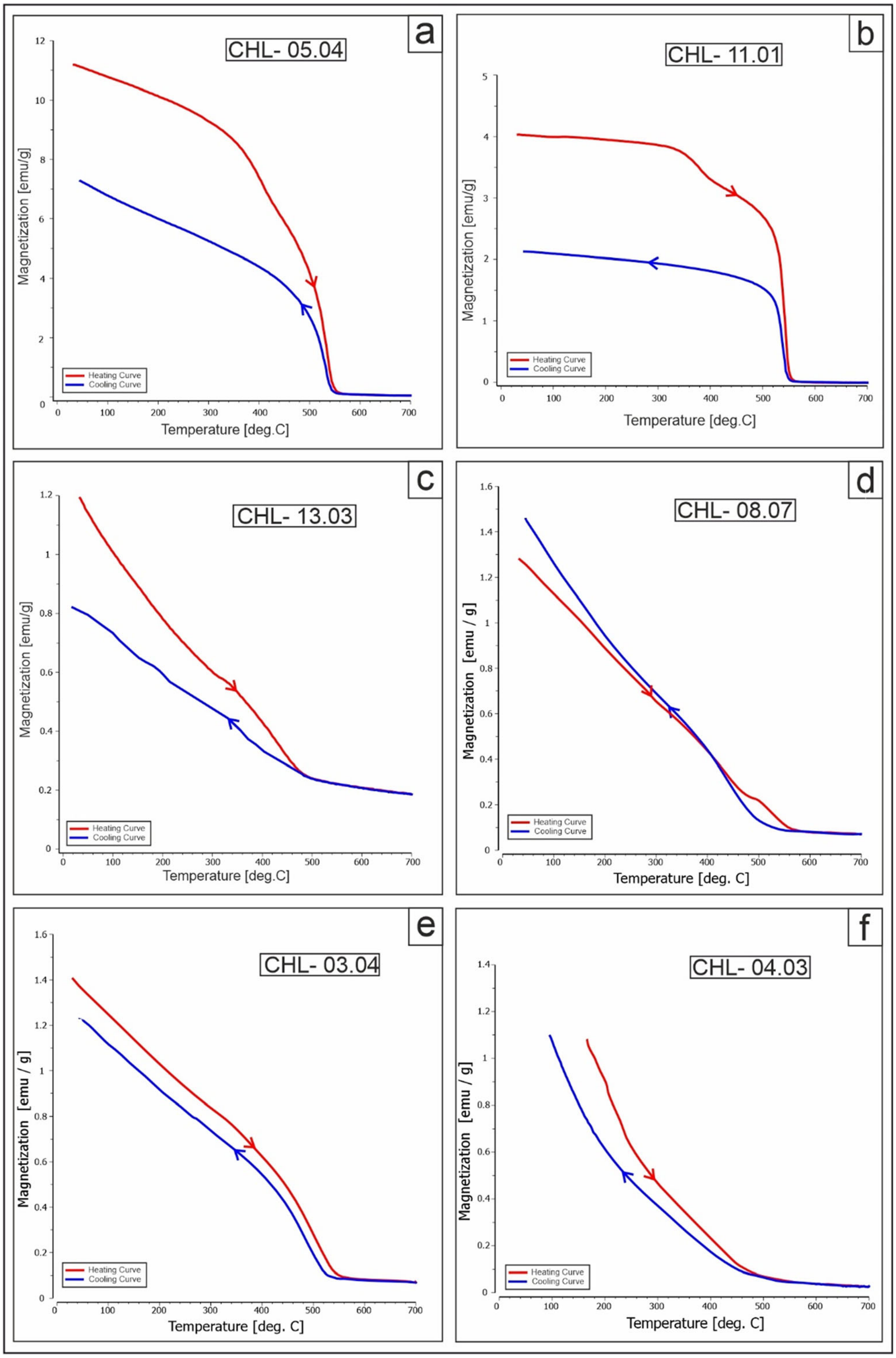

Figure 9. Thermomagnetic (magnetization vs. temperature) curves for representative samples.

oxides also suffered the retrograde path, i.e., the low-temperature oxidation, due to the presence of a corrugated grain boundary (figure 3c, d). There are three generations of Fe–Ti oxides present in the study area. Along the fractures of silicate grains (figure 5b) and along grain boundary (figure 5a), tiny magnetite grains are formed. Magnetite is identified due to the drop of the heating curve at Curie temperature $T_c \sim 580°C$ and that magnetite provides stable magnetization as the nature of the heating curve and the cooling curve is reversible (figure 9). The hysteresis curve, which shows

Table 1. *AMS parameters from samples from different sectors of different rock types.*

Site no.	No. of cores	K_1(D°/I°)	α_{95} for K_1	K_3 (D°/I°)	α_{95} for K_3	F	L	P_J	T_J	K_m ($\times10^{-6}$ CGS)
Northern sector granulites										
CHL 1	6	85.9/61.7	11.6	306.3/36.4	27.0	1.3	1.06	1.42	0.15	31.00
CHL 2	6	329.1/60.2	55.7	161.0/40.0	13.9	1.14	1.02	1.18	0.72	48.07
CHL 3	7	120.0/23.2	26	287.6/60.9	18.8	1.20	1.02	1.3	0.78	64.62
CHL 4	6	263.6/79.8	43.5	146.5/35.4	70.2	1.13	1.03	1.18	0.59	24.61
CHL 23	8	322/34.6	16.9	176.0/64.7	14.3	1.10	1.10	1.16	0.31	18.42
CHL 22	7	249.5/26.6	9.2	171.4/56.8	29.3	1.30	1.40	1.78	0.19	560.32
Mean		319.5/86.7		197.8/80.2		1.19	1.11	1.34	0.45	124.5
Southern sector granulites										
CHL 5	6	93.1/78.1	73.6	037.1/35.5	34.7	1.5	1.1	1.6	0.76	526.32
CHL 6	6	205.7/50.7	18	077.4/27.5	14.2	1.4	1.1	1.65	0.55	261.52
CHL 10	7	235/23	8.9	355.5/50.3	4.8	1.9	1.06	2.23	0.82	132.07
CHL 11	6	217.3/82.1	55.4	317.9/51.5	45.9	1.5	1.1	1.76	0.59	183.21
CHL 13	6	236.6/63.3	41.8	24.5/21.0	16.5	1.2	1.06	1.31	0.56	14.38
CHL 16	6	100/42.3	18.9	227.9/33.3	18.9	1.3	1.1	1.38	0.37	306.69
Mean		200.1/60.9		022.6/54.0		1.47	1.09	1.66	0.61	273.4
Anorthosite										
CHL 8	10	25.7/46.5	31.4	237.7/38.7	3.9	1.2	1.01	1.25	0.82	35.82
CHL 9	6	166.7/56.9	35.9	022.1/52.7	15.8	1.1	0.9	1.25	0.02	43.39
CHL17	7	323.7/62.6	39.4	103.2/39.7	43.3	1.3	1.3	1.89	0.02	3.37
CHL 17	7	219.7/79.1	38	333.6/40.7	46.6	1.3	1.2	2.59	0.16	14.43
CHL 19	11	100.3/43.3	35.2	218.6/23.9	11.5	1.2	1.1	1.27	0.44	18.47
CHL 20	13	142.1/49.	27.1	264.0/71.4	26.4	1.4	1.3	2.42	0.17	2.94
CHL 21	9	284.4/58.1	22.9	179.0/44.1	30.9	1.2	1.2	1.49	0.06	17.82
CHL 24	6	228.0/50.6	46.1	331.2/30.1	39	1.2	1.1	1.33	0.22	8.17
CHL 25	7	065.3/47.8	35	273.9/49.6	19.7	1.2	1.1	1.43	0.29	5.38
Mean		086.7/77.6		246.5/63.6		1.23	1.13	1.66	0.24	16.6
Leptynite										
CHL 7	6	359.2/7.21	50.2	250.6/31.4	22.3	1.2	1.1	1.39	0.26	12.49
CHL 12	7	152.6/64.6	60.6	129/33.2	29	1.2	1.1	1.3	0.35	18.71
CHL 14	7	257.2/56.9	27.8	118.6/55.8	21.7	1.3	1.2	1.54	0.38	9.75
CHL 15	7	308.3/63.7	46.4	101.0/19.2	37.7	1.1	1.02	1.2	0.69	19.41
Mean		249.7/78.1		150.3/40.6		1.2	1.11	1.36	0.42	15.09

saturation and remanence, indicates typical characterisation of the presence of ferrimagnetic magnetite (figure 6a, b, e, f; Soumya *et al.* 2017). The hysteresis curve of the samples CHL 13 and CHL 8 (figure 6c, d) shows little remanence, and the unsaturated nature indicates that in the studied rock samples, both ferrimagnetic and paramagnetic minerals are present. The Day plot indicates the chief magnetic remanence carrier belongs to fine-grained SD Ti-magnetites (figure 7). From the thermomagnetic study of the same sample, CHL 13, the presence of ferrimagnetic magnetite and paramagnetic haematite are observed (figure 9c). By the T_c and nature of the curve, paramagnetic haematite and ferrimagnetic magnetite are also identified (figure 9c). From the rock magnetic study, it is evident that ferrimagnetic magnetite and paramagnetic haematite are present (Satyanarayana *et al.* 2003).

5.2 *Magnetic fabric versus tectonics*

Orientation of the K_1 in the Chilka Lake area can serve as a proxy for the direction of the stress field during the different orogenic events of the EGMB. This is because the maximum susceptibility axes (K_1) align themselves along the direction of maximum elongation or the maximum extensional stress and evidently stay perpendicular to the direction of shortening or the maximum compressive stress (Goldstein 1980; Mondal *et al.* 2009;

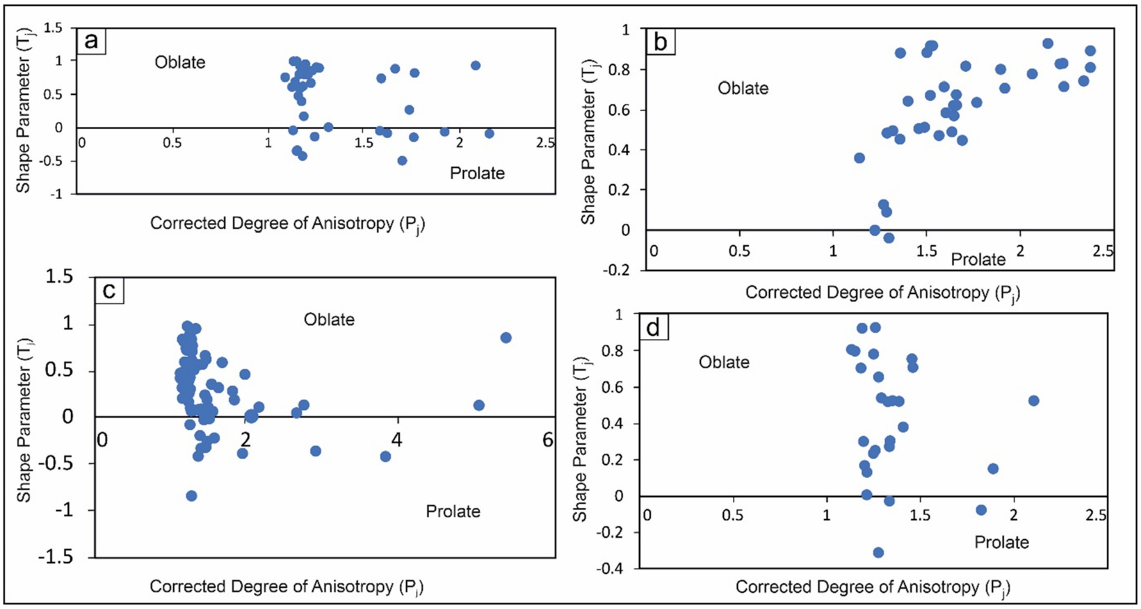

Figure 10. P_j vs. T_j plots for **(a)** northern sector granulites, **(b)** southern sector granulites, (**c**) anorthosite, and **(d)** leptynite.

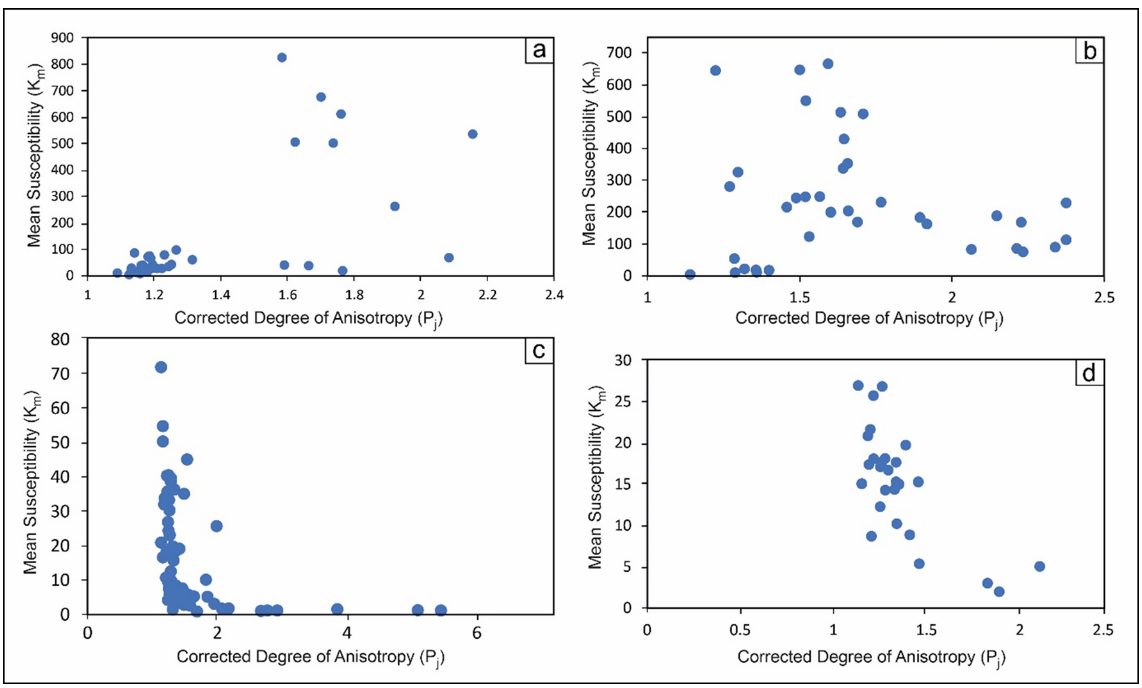

Figure 11. P_j vs. K_m plots for **(a)** northern sector granulites, **(b)** southern sector granulites, (**c**) anorthosite, and **(d)** leptynite.

Gain *et al.* 2022). Based on this the magnetic fabric development of the Chilka Lake area can be two staged, each having a relationship with a particular tectonic event in the terrain.

Stage 1 (metamorphism stage): Signature of the first stage in the development of magnetic fabric is recorded in the granulitic rocks of the area. These were the rocks which came into existence at the earliest among all ($\sim$2.0 Ga), where the signatures of the retreating phase of orogeny in the Eastern Ghats Belt, followed by subduction during 2–1.7 Ga is preserved (Dasgupta *et al.* 2013). Based on the orientation of the magnetic fabrics from granulite, the K_1 trends NE–SW mostly with some deviations in the southern granulite (figure 13a, b). This proves that during this stage, the distribution of the maximum compressional stress (σ_1) was oriented NE–SW, which is also parallel to the regional F_1 fold axis due to D_1 deformation.

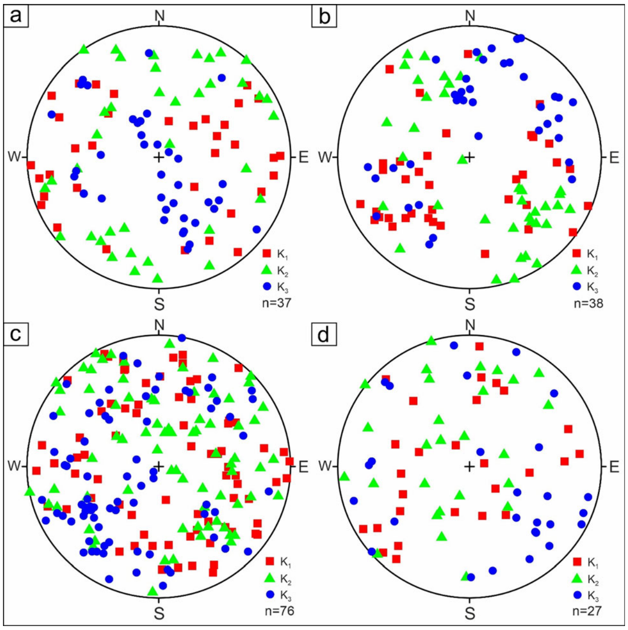

Figure 12. Lower hemisphere equal area plots for all the principal susceptibility axes for **(a)** northern sector granulites, **(b)** southern sector granulites, **(c)** anorthosite, and **(d)** leptynite.

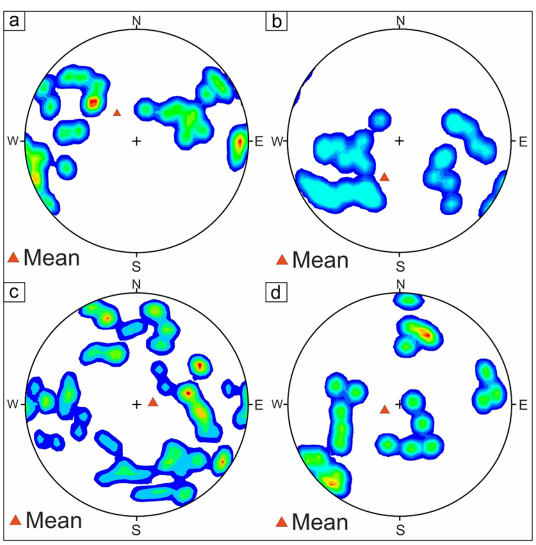

Figure 13. Lower hemisphere equal area plots for the magnetic lineation for **(a)** northern sector granulites, **(b)** southern sector granulites, **(c)** anorthosite, and **(d)** leptynite.

However, the magnetic foliation plane developed during this stage is not parallel to the regional schistosity. This reversal in the magnetic fabric away from the mesoscopic one may be due to the high susceptibility magnetite, which is developed during this stage only because of UHT metamorphism in this phase (Sengupta *et al.* 1999; Dasgupta *et al.* 2013). High-susceptibility magnetite

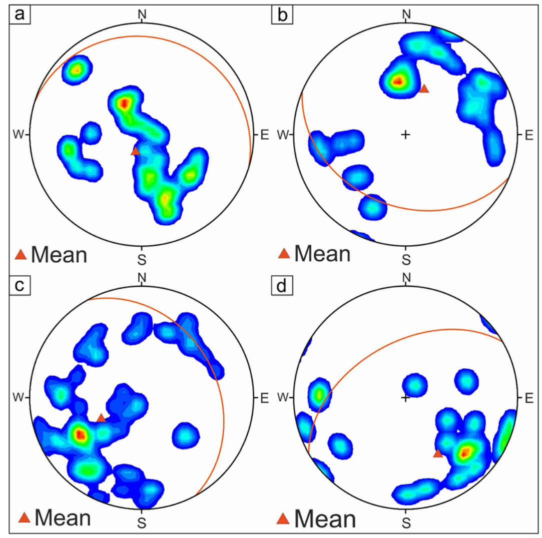

Figure 14. Lower hemisphere equal area plots showing the magnetic foliation for **(a)** northern sector granulites, **(b)** southern sector granulites, **(c)** anorthosite, and **(d)** leptynite.

grains have the capability of rotating the magnetic foliation plane in the direction of mineral growth, deviating it from the mesoscopic schistosity. A certain degree of positive correlation between P_j and K_m in both the granulites of southern and northern sectors speaks for the same (figure11a, b).

Stage 2 (magmatism stage): An analogy with the maximum susceptibility axes as a proxy from this σ_1 orientation in the anorthosite and leptynite as well, which are the products of post-subduction magmatism, it is noted that the stress field orientation was not constant.

Initially, in the metamorphism stage, the σ_1 orientation was NE–SW, which is still somewhat preserved in the magnetic lineation of leptynite, which finally grades to an E–W orientation, and it becomes completely haphazard in the anorthosite. Hence, the leptynite marks the transition between the metamorphism and final magmatism stage. Hence, based on the magnetic fabrics, the leptynites are prior to anorthosite. Mesoscopically also, the D1 and D2 signatures are absent in the anorthosites, and the E–W orientation of the K_1 fabric in leptynites is in accordance with the D_3 deformation. The felsic magmatism, mainly the anorthosites, have unoriented magnetic fabrics without preserving the regional tectonics because the anorthosites were emplaced after the completion of the D_3 phase of deformation, after the emplacement of the leptynites.

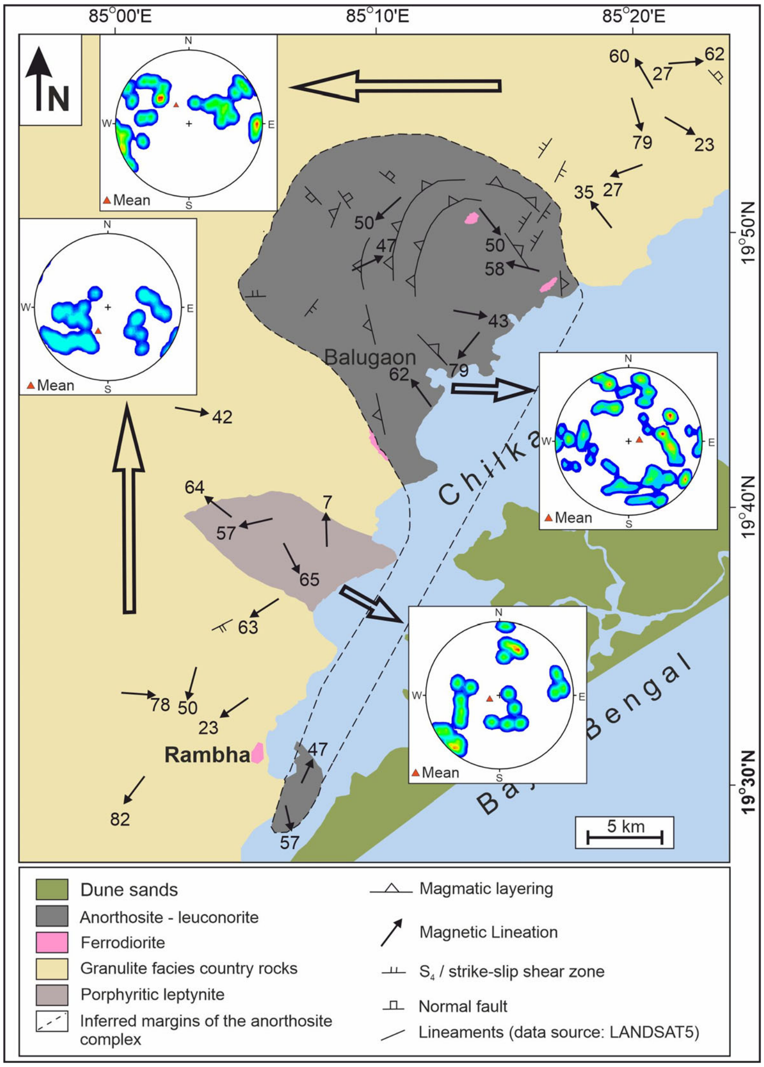

Figure 15. Magnetic lineation distribution of the study area. Different sector plots are shown in individual equal-area diagrams.

6. Conclusions

From the rock magnetic study, it is clear that the ferrimagnetic character and the magnetic remanence carrier of the studied rocks are Ti-magnetite and haematite. The rocks are rich in Ti-magnetite because of their prolonged metamorphism to granulite (Frost and Shive 1986; Shive and Fountain 1988; Shive *et al.* 1992; Liu *et al.* 2013). Progressive metamorphism to granulite facies increases the amount of ferrimagnetic Ti-magnetite and magnetite. Conversely, retrogration imprints paramagnetic contents (Wang *et al.* 2015). In the present case, the scenario is the same here, due to retrograde metamorphism (Sengupta *et al.* 1999) in the rock's paramagnetic character. The metamorphism took place in the rocks that came into existence ($\sim$2.0 Ga), and the following orogeny signatures are captured in the granulites. Based on magnetic fabrics, magnetic lineation trends NE–SW in the granulites, with some exceptions in the southern granulites. This is followed by magmatic events, which are experienced by leptynite, whose K_1 trends from NE–SW to E–W. Then comes the anorthosite where there is no such magnetic fabric orientation.

Acknowledgements

Solanky Das thankfully acknowledges the Jadavpur University for providing the funds under the NON-NET Fellowship for the field and laboratory analysis and the Department of Geological Sciences, Jadavpur University, for providing high-resolution microscopes in the image analyser laboratory used in the microstructural study. The author thanks the Director, CSIR-NGRI,

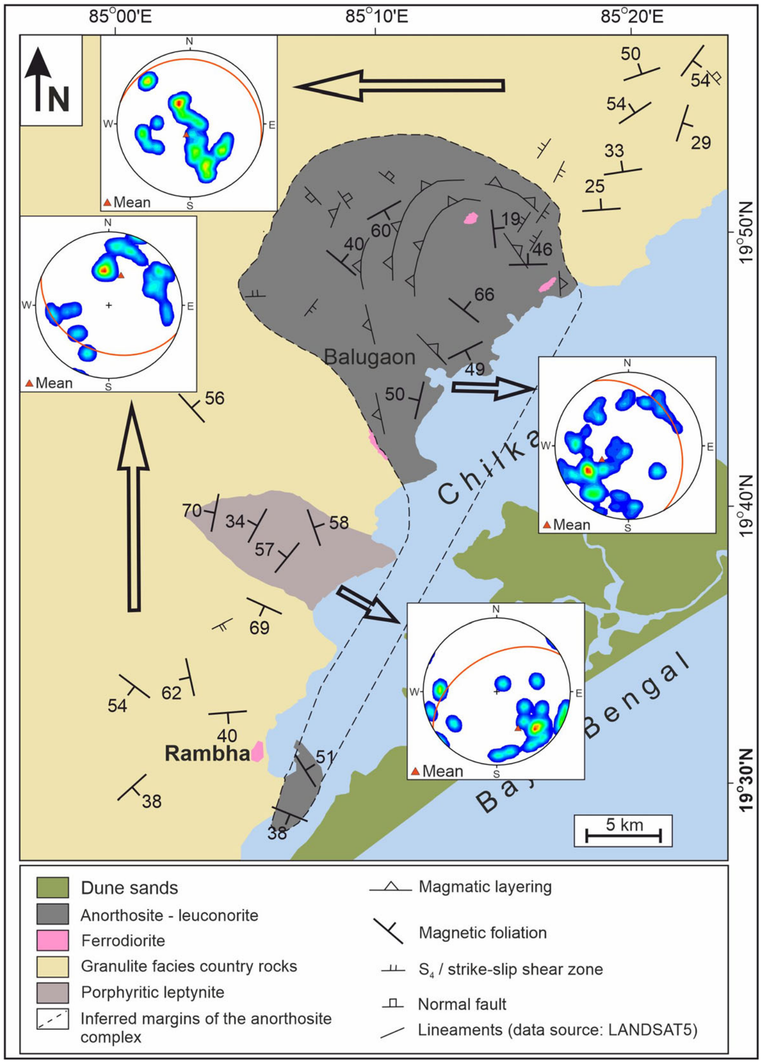

Figure 16. Magnetic foliation distribution of the study area. Different sector plots are shown in individual equal-area diagram.

Hyderabad, for giving permission for the different rock magnetic analyses.

Author statement

Solanky Das: Manuscript writing, data curation, investigation, and formal analysis. M Venkateshwarlu: Sample analysis. Supriya Mondal: Formal analysis and supervision. Saurodeep Chatterjee: Data curation, formal analysis and manuscript writing. Debesh Gain: Data curation and formal analysis.

References

Agarwal A, Srivastava D C, Shah J and Mamtani M A 2021 Magnetic fabrics in an apparently undeformed granite body near Main Boundary Thrust (MBT), Kumaun Lesser Himalaya, India; *Tectonophys.* **815(228)** 996, https://doi.org/10.1016/j.tecto.2021.228996.

Akimoto T, Kinoshita H and Furuta T 1984 Electron probe microanalysis study on process of low temperature oxidation of titano-magnetite; *Earth Planet. Sci. Lett.* **71** 263–278.

Anderson A T Jr 1969 Massif type anorthosite: A widespread Precambrian igneous rock; In: Origin of anorthosite and related rocks (ed.) Isachsen Y W, *N.Y. State Mus, Sci. Ser. Mem.* **18** 47–56.

Berrang J P 1996 Some critical differences between orogenic plutonic and gravity-stratified anorthosites; *Geol. Rundsch.* **55** 617–642.

Bhattacharya A, Raith M, Hoernes S and Banerjee D 1998 Geochemical evolution of the massif-type anorthosite complex at Bolangir in the Eastern Ghats Belt of India; *J. Petrol.* **39** 1169–1195.

Borradaile G J 1991 Correlation of strain with anisotropy of magnetic susceptibility (AMS); *Pure Appl. Geophys.* **135** 15–29.

Borradaile G J and Alford C 1987 Relationship between magnetic susceptibility and strain in laboratory and experiments; *Tectonophys.* **133** 121–135.

Brown L L and McEnroe S A 2004 Paleomagnetism of the Egersund–Ogna anorthosite, Rogaland, Norway, and the position of Fennoscandia in the Late Proterozoic; *Geophys. J. Int.* **158** 479–488.

Brown L L and McEnroe S A 2012 Paleomagnetism and magnetic mineralogy of Grenville metamorphic and igneous rocks, Adirondack Highlands, USA; *Precamb. Res.* **212–213** 57–74.

Brown L L and McEnroe S A 2008 Magnetic properties of anorthosites: A forgotten source for planetary magnetic anomalies; *Geophys. Res. Lett.* **35** L02305, https://doi.org/10.1029/2007GL032522.

Chatterjee S C 1960 The problem of the anorthosites with special reference to the anorthosites of Bengal; *Proc. 46th Ind. Sci. Cong. Pt-II.*

Chatterjee S, Mondal S, Gain D, Baidya T K and Mazumdar D 2018a Interpretation of magnetic fabrics in the Dalma volcanic rocks and associated metasediments of the Singhbhum mobile belt; *J. Earth Syst. Sci.* **127(11)** 89.

Chatterjee S, Mondal S, Roy P, Gain D and Bhattacharya A 2018b Magneto-mineralogical characterization and manifestations of magnetic fabrics from the gneissic rocks and associated intrusive bodies in and around Bankura and Purulia districts, West Bengal, India; *Curr. Sci.* **114(9)** 1894–1902.

Das K, Bose S, Karmakar S and Chakraborty S 2012 Petrotectonic framework of granulites from northern part of Chilka Lake area, Eastern Ghats Belt, India: Compressional vis-á-vis transpressional tectonics; *J. Earth Syst. Sci.* **121(1)** 1–17.

Dasgupta S, Bose S and Das K 2013 Tectonic evolution of the eastern Ghats Belt, India; *Precamb. Res.* **227** 247–258.

De A 1969 Anorthosites of the Eastern Ghats, India; In: *Origin of anorthosite and related rocks, N.Y. State Mus* (eds) Isachsen Y W, *Sci. Ser. Mem.* **18** 425–434.

Day R, Fuller M and Schmidt V A 1977 Hysteresis properties of titanomagnetites: Grain size and compositional dependence; *Phys. Earth Planet. Int.* **13** 260–267.

Dobmeier C J and Raith M M 2003 Crustal architecture and evolution of the Eastern Ghats Belt and adjacent regions of India; In: Proterozoic East Gondwana: Supercontinent assembly and beak up (eds) Yoshida M, Windley B F and Dasgupta S, *Geol. Soc. London, Spec. Publ.* **206** 145–168.

Dobmeier C and Simmat R 2002 Post-Grenvillean transpression in the Chilka Lake area, Eastern Ghats Belt – implications for the geological evolution of peninsular India; *Precamb. Res.* **113** 243–268.

Dvorak J and Hrouda F 1975 The reflection of the deeper structure of the Artmanovosoblaha block (Nizky Jesenik Mountains, Czechoslovakia) in the magnetic anisotropy and deformation history of overlying palaeozoic sediments; *Vest. Ustred. Ust. Geol.* **50** 285–296.

Ferré E C, Gébelin A, Till J L, Sassier C and Burmeister C K 2014 Deformation and magnetic fabrics in ductile shear zones: A review; *Tectonophys.* **629** 179–188.

Fodor L I, Marton E, Vrabec M, Koroknai B, Trajanova M and Vrabec M 2020 Relationship between magnetic fabrics and deformation of the Miocene Pohorje intrusions and surrounding sediments (Eastern Alps); *Int. J. Earth Sci. (Geol. Rundsch.)* **109** 1377–1401, https://doi.org/10.1007/s00531-020-01846-4.

Frost B R and Shive P N 1986 Magnetic mineralogy of the lower continental crust; *J. Geophys. Res.* **91** 6513–6521.

Gain D, Chatterjee S and Mondal S 2022 Rock magnetism and AMS studies in Kondapalle–Pangidi layered complex, Eastern Ghats Belt, India: Remanence carriers and tectonic implications; *Phys. Earth Planet. Int.* **329–330** 106910.

Goldstein A G 1980 Magnetic susceptibility anisotropy of mylonites from the Lake Char mylonite zone, southeastern New England; *Tectonophys.* **66(1–3)** 197–211.

Haggerty S E 1976a Oxidation of opaque mineral oxides in basalts; In: Oxide Minerals (ed.) D Rumble, *Mineral. Soc. Am.* Short Course Notes, No. 3, Hg1–Hg100.

Isachsen Y W 1969 Origin of anorthosite and related rocks – a summarisation; In: Origin of anorthosite and related rocks (ed.) Isachsen Y W, *N.Y. State Mus., Sci. Ser. Mem.* **18**.

Jelinek V 1981 Characterisation of the magnetic fabrics of rocks; *Tectonophys.* **79** 63–67.

Johnson H P and Hall J M 1978 A detailed rock magnetic and opaque mineralogy study of the basalts from Nazca Plate; *Geophys. J. Roy. Astron. Soc.* **52** 45–64.

Krause O, Dobmeier C, Raith M M and Mezger K 2001 Age of emplacement of massif-type anorthosites in the Eastern Ghats Belt, India: Constraints from U–Pb zircon dating and structural studies; *Precamb. Res.* **109** 25–38.

Liu Q S, Wang H C, Zheng J P, Zeng Q L and Liu Q S 2013 Petromagnetism properties of granulite-facies rocks from the northern North China craton: Implications for magnetic and evolution of the continental lower crust; *J. Earth Sci.* **24** 12–28.

McEnroe S A, Harrison R J, Robinson P and Langen Horst F 2002 Nanoscale haematite–ilmenite lamellae in massive ilmenite rock: An example of lamellar magnetism with implications for planetary magnetic anomalies; *Geophys. J. Int.* **151** 890–912.

Mondal S, Piper J D A, Hunt L, Bandopadhyay G and Basu Mallick S 2009 Palaeomagnetic and rock magnetic study of charnockites from Tamil Nadu, India and the 'Ur' protocontinent in early Palaeoproterozoic times; *J. Asia Earth Sci.* **34(493)** 506.

Mondal T K, Chowdhury A, Sain A and Chatterjee S 2022 Understanding the maturity of columnar joints and its spatial relationship with eruptive centre: A critical appraisal from the Rajmahal Basalt, India; *Phys. Earth Planet. Int.* **326** 106867.

Parés J M and van der Pluijm B A 2002 Evaluating magnetic lineations (AMS) in deformed rocks; *Tectonophys.* **350** 283–298.

Perraju P 1960 Occurrence of anorthosite in Puri district, Orissa; *Ind. Minerals* **14** 310.

Perraju P 1973 Anorthosite of Puri district, Orissa; *Rec. Geol. Surv. India* **105, Pt-2** 102–116.

Ray C 1952 Anorthosite in Chilka Lake; *Proc. Ind. Sci. Cong. 39th Sess. Pt-3,* 177 (abs).

Robinson P, Harrison R J, McEnroe S A and Hargraves R B 2002 Lamellar magnetism in the haematite–ilmenite series as an explanation for strong remanent magnetization; *Nature* **418** 517–520.

Robinson P, Harrison R J, McEnroe S A and Hargraves R B 2004 Nature and origin of lamellar magnetism in the hematite–ilmenite series; *Am. Mineral.* **89** 725–747.

Satyanarayana K V V, Arora B R and Janardhan A S 2003 Rock magnetism and palaeomagnetism of the

Oddanchatram anorthosite, Tamil Nadu, South India; *Geophys. J. Int.* **155(3)** 1081–1092.

Sen S K 1987 Origin of leptynite, an orthopyroxene-free granite-gneiss, in two granulite terrains of India; *Recent Res. Geol.* **13** 117–124.

Sengupta P, Sen J, Dasgupta S, Raith M, Bhui U K and Ehl J 1999 Ultra-high temperature metamorphism of metapelitic granulites from Kondapalle, Eastern Ghats Belt: Implications for the Indo-Antarctic correlation; *J. Petrol.* **40(7)** 1065–1087.

Shive P N, Blakely R J, Frost B R and Fountain D M 1992 Magnetic properties of the lower continental crust; In: *Continental Lower Crust* (eds) Fountain D M, Arculus R, Kay R W, Elsevier, pp. 145–178.

Shive P N and Fountain D M 1988 Magnetic mineralogy in an Archean crustal cross section: implications for crustal magnetization; *J. Geophys. Res.* **93** 12,177–12,186.

Sighinolfi G P and Gorgoni C 1975 Genesis of massif-type anorthosites – the role of high grade metamorphism; *Contrib. Mineral. Petrol.* **51** 119–126.

Soumya G S, Asanulla R M and Radhakrishna T 2017 Rockmagnetism in relation to magnetic mineralogy of anorthosites in the southern granulite region of the Indian shield; *Geophys. J. Int.* **209(3)** 1768–1778.

Tarling D and Hrouda F 1993 *Magnetic anisotropy of rocks*; Springer, pp. 14–27.

Till J L, Jackson M J and Moskowitz B M 2010 Remanence stability and magnetic fabric development in synthetic shear zones deformed at 500°C; *Geochem. Geophys. Geosyst.*, https://doi.org/10.1029/2010GC003320.

Walker T L 1902 Geology of Kalahandi State, Central Provinces; *Geol. Surv. India Memoir* **33** 1–22.

Wang H, Liu Q, Zhao W, Li Z and Zheng J 2015 Magnetic properties of Archean gneisses from the northeastern North China Craton: The relationship between magnetism and metamorphic grade in the deep continental crust; *Geophys. J. Int.* **201** 486–495.

Corresponding editor: N V Chalapathi Rao